Available online at www.sciencedirect.com

SCIENCE DIRECT

Developmental Biology 274 (2004) 171–187

DEVELOPMENTAL BIOLOGY

www.elsevier.com/locate/ydbio

Regionalization of cell fates and cell movement in the endoderm of the mouse gastrula and the impact of loss of *Lhx1(Lim1)* function

Patrick P.L. Tam[a,*], Poh-Lynn Khoo[a], Nicole Wong[a], Tania E. Tsang[a], Richard R. Behringer[b]

[a]*Embryology Unit, Children's Medical Research Institute, University of Sydney, New South Wales, Australia*
[b]*Department of Molecular Genetics, MD Anderson Cancer Center, University of Texas, Houston, Texas, USA*

Received for publication 8 May 2004, revised 1 July 2004, accepted 2 July 2004
Available online 8 August 2004

Abstract

Investigation of the developmental fates of cells in the endodermal layer of the early bud stage mouse embryo revealed a regionalized pattern of distribution of the progenitor cells of the yolk sac endoderm and the embryonic gut. By tracing the site of origin of cells that are allocated to specific regions of the embryonic gut, it was found that by late gastrulation, the respective endodermal progenitors are already spatially organized in anticipation of the prospective mediolateral and anterior–posterior destinations. The fate-mapping data further showed that the endoderm in the embryonic compartment of the early bud stage gastrula still contains cells that will colonize the anterior and lateral parts of the extraembryonic yolk sac. In the *Lhx1(Lim1)*-null mutant embryo, the progenitors of the embryonic gut are confined to the posterior part of the endoderm. In particular, the prospective anterior endoderm was sequestered to a much smaller distal domain, suggesting that there may be fewer progenitor cells for the anterior gut that is poorly formed in the mutant embryo. The deficiency of gut endoderm is not caused by any restriction in endodermal potency of the mutant epiblast cells but more likely the inadequate allocation of the definitive endoderm. The inefficient movement of the anterior endoderm, and the abnormal differentiation highlighted by the lack of *Sox17* and *Foxa2* expression, may underpin the malformation of the head of *Lhx1* mutant embryos.

Keywords: Endoderm; Cell fate; Cell movement; *Lhx1* function; Gastrulation; Mouse

Introduction

Gastrulation is a major milestone in mouse development when the three embryonic germ layers are formed. The establishment of progenitor cell populations of major tissue lineages is heralded by the acquisition of diverse fates by cells localized in different regions of the germ layers. Regionalization of cell fate and tissue patterning are the fundamental components of the blueprint of embryonic development. This blueprint, or the body plan, carries essential information of the status of determination of the lineage progenitors and their geographical location with reference to the anterior–posterior, mediolateral, and dorsoventral embryonic axes (Tam and Behringer, 1997). The latter information can be depicted as a series of fate-maps of the germ layers at gastrulation and their derivatives at early organogenesis. In these fate-maps, the localization of the progenitor cells and their descendants is charted at successive stages of development. These data provide not only a visualization of tissue patterning but also enable the reconstruction of the pattern of morphogenetic movement of cells during embryonic development. The pattern of cell movement may illustrate how tissue components of specific body parts or organs can be assembled to bring about inductive interaction and allow organogenesis to proceed (Tam et al., 2001).

Useful insights into the cellular and molecular mechanisms of embryonic patterning have been gained by analyzing the impact of loss of specific gene function on

* Corresponding author: Embryology Unit, Children's Medical Research Institute, University of Sydney, Locked Bag 23, Wentworthville, NSW 2145, Australia. Fax: +61 2 9687 2120.
E-mail address: ptam@cmri.usyd.edu.au (P.P.L. Tam).

0012-1606/$ - see front matter © 2004 Elsevier Inc. All rights reserved.
doi:10.1016/j.ydbio.2004.07.005

developmental processes such as gastrulation and early organogenesis. The mouse LIM domain containing gene, *Lhx1(Lim1)*, has been shown to play an essential role in the development of head structures in the mouse (Shawlot and Behringer, 1995). Loss of *Lhx1* activity in the visceral endoderm, primitive streak, nascent mesoderm, and the mesendodermal derivatives of the gastrula organizer results in abnormal morphogenesis of the gastrula embryo (Figs. 1A and B) and the truncation of the head culminating in the loss of craniofacial structures that are rostral to the upper hindbrain (Shawlot and Behringer, 1995). Analysis of the expression of tissue-specific molecular markers revealed that the primitive streak and the prospective gastrula organizer are localized ectopically and the presumptive anterior–posterior embryonic axis, which is aligned with the proximal–distal axis of the pregastrulation embryo initially, fails to reorient to the transverse plane of the gastrula embryo (Kinder et al., 2001a; Shawlot and Behringer, 1995). Lacking *Lhx1* activity therefore impacts significantly on the early patterning of the mouse embryo.

Chimera analysis using reciprocal combinations of host embryo and embryonic stem cells of wild-type and *Lhx1−/−* genotype has shown that *Lhx1* function is required autonomously in both the extraembryonic tissues (principally the visceral endoderm) and the epiblast derivatives, especially the anterior mesendoderm, for anterior patterning (Shawlot et al., 1999). In the mouse chimera, *Lhx1−/−* cells can colonize the epiblast of the gastrula extensively and their descendants could be found in the derivatives of all three germ layers. In chimeras displaying a strong presence of the *Lhx1−/−* cells, mutant cells were present in the anterior axial mesendoderm and the cranial paraxial mesoderm, which play a critical role in neural induction (Ang and Rossant, 1993; Camus et al., 2000) and neural tube morphogenesis (Chen and Behringer, 1995). These chimeras did not develop normally and manifested anterior defects that become more severe with the increase in the population of mutant cells in the primitive streak-derived embryonic tissue (Shawlot et al., 1999). This finding provides compelling genetic evidence that head formation requires sequential inductive interaction with first the visceral endoderm (Beddington and Robertson, 1999; de Souza and Niehrs, 2000) and later the anterior mesendoderm derived from the gastrula organizer and/or the primitive streak (Beddington, 1994; Camus and Tam, 1999; Camus et al., 2000; Kinder et al., 2001b).

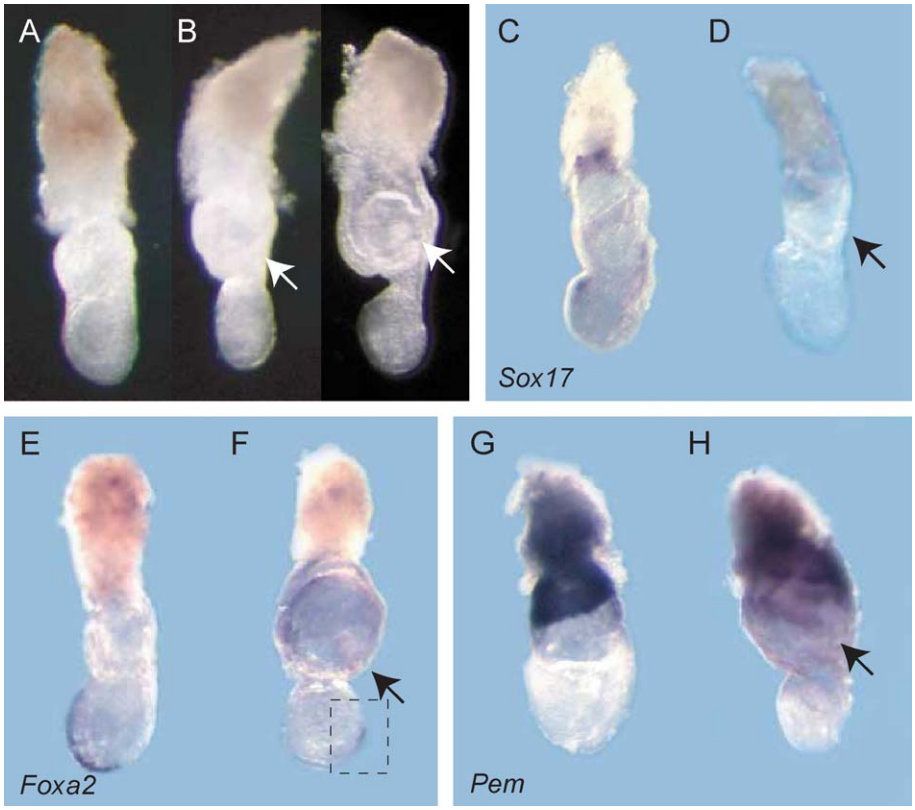

Fig. 1. (A) A wild-type E7.5 no-bud stage embryo. (B) Two *Lhx1−/−* E7.5 mutant gastrula stage embryos showing the disproportionately small embryonic size and the deficiency of anterior germ layer tissues. (C–H) Expression of (C and D) *Sox17*, (E and F) *Foxa2*, and (G and H) *Pem* in wild-type (C, E, and G) and *Lhx1−/−* mutant embryos (D, F, and H). *Sox17* expression is absent in all five *Lhx1−/−* embryos examined, *Foxa2* is expressed in the posterior region in three of four *Lhx1−/−* embryos examined (one shows no expression), and *Pem* is expressed in the extraembryonic endoderm and the chorion all four *Lhx1−/−* embryos examined. Black arrows indicate the structure that resembles the allantoic bud or its primordium, which identifies the prospective posterior side of the embryo. The box in F shows the region from which fragments were isolated for the transplantation experiments. The fragment contains the posterior epiblast, part of the primitive streak, and the presumptive gastrula organizer.

The unrestricted ability of the *Lhx1−/−* cells to colonize tissues derived from all three germ layers (Shawlot et al., 1999) suggests that loss of *Lhx1* function does not affect the developmental potency of the epiblast cells. Lineage potency has also been tested by transplanting *Lhx1−/−* epiblast cells into the primitive streak and the prospective neural plate of wild-type host embryos. The finding reveals that *Lhx1* activity is not required for the allocation of cells to the cranial neuroectoderm, the lateral plate mesoderm, and the paraxial mesoderm (Hukriede et al., 2003; Shawlot et al., 1999; Tsang et al., 2000). *Lhx1−/−* cells, however, are unable to activate lateral mesoderm-specific gene activity, even when they have been incorporated into the wild-type lateral mesoderm of the host embryo (Tsang et al., 2000). Further demonstration of the impact of *Lhx1* function on tissue differentiation was shown by the reduction of the primordial germ cell population and the deficiency of the allantoic mesoderm in *Lhx1−/−* embryos (Tsang et al., 2001). *Lhx1−/−* cells also fail to participate fully in the morphogenetic movement of the lateral and paraxial mesoderm after ingression at the primitive streak (Hukriede et al., 2003; Tsang et al., 2000). Loss of *Lhx1* activity leads to the down-regulation of *Amot* in the visceral endoderm (Shimono and Behringer, 1999). *Amot* function has recently been shown to be essential for the displacement of the visceral endoderm from the anterior region of the pre- and early streak embryo to the extraembryonic site (Shimono and Behringer, 2003). Although *Lhx1* is not expressed in the definitive endoderm that gives rise to the gut endoderm, it would be of interest to find out if migration of the definitive endoderm may also be impeded in the presence of disrupted movement of the visceral endoderm.

Lhx1−/− epiblast-derived cells are found in the endoderm of chimeras that are populated by large number of mutant cells (Shawlot et al., 1999). In this regard, the strong chimera is almost equivalent to the null-mutant embryo (Shawlot and Behringer, 1995). The presence of endoderm-like cells in the strong chimera and the null-mutant embryo suggests that loss of *Lhx1* function may not affect the allocation of the endoderm lineage. However, cells in the endodermal layer of the null-mutant embryo do not express *Sox17*, *Foxa2*, *Shh*, and *Cerl* appropriately (Kinder et al., 2001a; Shawlot and Behringer, 1995; Shawlot et al., 1999; Figs. 1C–F). The lack of expression of endodermal markers raises the possibility that the null-mutant embryo is deficient of definitive endoderm or that the endoderm-like cells do not differentiate properly. In contrast, *Pem* expression appears normal in the *Lhx1*-null mutant (Figs. 1G and H), indicating that differentiation of the extraembryonic endoderm may be unaffected. Although the outcome of chimera analysis and the null-mutant phenotype are consistent with the concept that *Lhx1* function is not essential for endoderm formation, there may be subtle defects in the potency of cells to differentiate into endoderm of specific parts of the embryonic gut. It would therefore be pertinent either to assess the endodermal contribution by mutant cells in chimeras displaying moderate to low contribution of the *Lhx1−/−* embryonic stem cells or to test more specifically the endodermal potency of endodermal progenitors in the epiblast of the *Lhx1−/−* gastrula.

The study reported in this paper was undertaken to investigate the impact of *Lhx1* function on three key aspects of endodermal development in the mouse: the lineage potency of the epiblast cell population, the patterning of the endoderm at gastrulation, and the morphogenetic tissue movement during gut formation. In addition, a significant outcome of this study is the provision of a complete description of the cell fates of the endoderm of the mouse embryo at late gastrulation and the insights into the pattern of cell movement that accompanies the formation of the embryonic gut.

Materials and methods

Mouse strains

Lhx1+/− mutant mice (Shawlot and Behringer, 1995) were mated to obtain embryos of wild-type, heterozygous, and homozygous mutant genotypes. The wild-type and *Lhx1+/−* embryos were indistinguishable morphologically at gastrulation to early somite stages and both the wild-type and *Lhx1+/−* mice develop normally to adulthood (Shawlot and Behringer, 1995). In the present study, they were grouped together as "normal" embryos on the basis of their phenotypic similarity. *Lhx1−/−* embryos, which could be distinguished from the normal embryos by their abnormal morphology (Figs. 1A and B), were called "null-mutant" embryos. These embryos were used for the fate-mapping experiments.

A new stock of *Lhx1+/−;EGFP;lacZ* mice of a mixed 129, C57BL6, DBA/2, and CD1 background was produced by crossing *Lhx1+/−* mice with transgenic mice that express *Hmgcr–lacZ* (Tam and Tan, 1992) and CMV–βactin–EGFP (Hadjantonakis et al., 1998). The *Lhx1+/−;EGFP;lacZ* mice were intercrossed to produce wild-type, *Lhx1+/−*, and *Lhx1−/−* embryos that also express the EGFP and the *lacZ* transgenes widely in all cell types. These normal and null-mutant embryos were the donors of cells and tissues for the cell and tissue transplantation experiments. Wild-type ARC/s strain embryos were used as recipients (hosts) of the transplantation.

Whole mount in situ hybridization

Embryos were processed for in situ hybridization analysis for the expression of *Pem*, *Sox17*, and *Foxa2* according to the protocol of Wilkinson and Nieto (1993) with the following modifications: Riboprobes were labeled with digoxigenin-11-UTP (Roche) using the AmpliScribe kit (Epicentre Technologies), SDS was used in place of CHAPS in both prehybridization and hybridization, no RNA digestion was performed after hybridization, and formamide was omitted from posthybridization washes.

Introduction of expression vectors by whole embryo electroporation

Normal no- to early bud stage embryos and the null-mutant littermates were harvested from *Lhx1+/−* mice for fate-mapping the endoderm. Marking of the endodermal cells at specific sites was performed by electroporation. The embryos were soaked for 5 min in aqueous plasmid DNA solution containing either 1–1.5 μg/μl *CMV–EGFP* expression vector or with equal concentrations of the *CMV–EGFP* and *Hmgcr–lacZ* expression vectors. The endoderm of the embryo was electroporated following the protocol of Davidson et al. (2003) and cultured in vitro (Sturm and Tam, 1993). The sites of electroporation were ascertained by the localization of the EGFP-expressing cells 3 h after electroporation and recorded by digital photography. At the end of 24 h of in vitro culture, the distribution of the EGFP-expressing cells was recorded. The number of EGFP-expressing cells was scored in high-magnification digital images of the embryo. When cells were clustered, an approximate number is estimated based on the size of the EGFP spot for individual cells. The score for some specimens was therefore was not an absolute count. The data were presented as the relative abundance of the labeled cells in defined regions of the yolk sac and the embryo (see later) to the nearest 5th percentile of the total cell population. The mean percentage for each region was then computed for specimens of the same electroporation site. Altogether, 86 wild-type and *Lhx1+/−* embryos were electroporated and 68 (79%) developed to early somite stage after 24 h of culture and contained EGFP-expressing cells in the endoderm. Embryos were excluded from this study when the initial electroporation did not produce a localized labeling of the endodermal cells. Of the *Lhx1−/−* mutant embryo, 83 were electroporated and 56 (67%) were analyzable after in vitro culture. That more embryos were excluded was due primarily to the higher incidence of poor embryonic growth and abnormal morphogenesis, which hampered a proper mapping of the distribution of EGFP-expressing endodermal cells.

Selected wild-type embryos that have been co-electroporated with EGFP and *lacZ* expression vectors were fixed for 2–3 min in 4% paraformaldehyde after the pattern of distribution of EGFP-expressing cells was recorded. They were stained by X-gal solution overnight at 37°C. The embryos were then processed and embedded in paraffin wax and sectioned at 8 μm. The sections were counterstained with Nuclear Fast Red and mounted in Canada balsam. The *lacZ*-expressing cells were identified by the blue X-gal staining reaction.

Isolation and transplantation of cells and tissues

Pregnant *Lhx1+/−;EGFP;lacZ* mice were euthanized at E7.0–7.5 to harvest embryos for isolating donor tissues for transplantation. Tissue fragments were dissected from the anterior region of the primitive streak of the midstreak stage normal embryo. From the null-mutant embryo, tissue fragments were isolated from the posterior region that includes the domain of *Chrd* and *Foxa2* expression (Kinder et al., 2001a; Figs. 1E and F) and part of the primitive streak (based on previous finding on *Wnt3*, *Fgf8*, and *T* expression; Kinder et al., 2001a). The embryonic fragments were trimmed to remove the mesoderm and endoderm, leaving only the epiblast/ectoderm, and further dissected into smaller clumps of about 10–15 cells. These clumps were transplanted using a Leica micromanipulator into either the anterior primitive streak region of wild-type midstreak (E7.0) stage or to the primitive streak immediately posterior to the node of the no- to early bud (E7.5) stage ARC/s host embryos (Kinder et al., 2001b). The host embryos were examined by fluorescence microscopy 1 h after transplantation to ascertain the location of the EGFP-expressing graft. Embryos showing incorrect positioning of the graft were excluded from further analysis.

For studying the morphogenetic behavior of the tissues, fragments of the anterior primitive streak of midstreak stage normal embryos and the posterior epiblast tissue of the null-mutant embryo were trimmed to isolate fragments containing about 50–80 cells. They were transplanted as an intact piece to the lateral site of the no- to early bud E7.5 ARC/s host embryo (Beddington, 1994; Tam and Steiner, 1999). For comparison, the node of late-streak stage normal embryos was also isolated and transplanted to the same site in the no- to early bud E7.5 ARC/s host embryos.

Host embryos and the remainder of the donor embryos were cultured together in rolling bottles as previously described (Sturm and Tam, 1993) for 24 h until the embryo reached the 6–8 somite stage. The host embryos were examined by fluorescence microscopy to visualize the distribution of the graft-derived EGFP-expressing cells. Embryos were then briefly fixed in 4% paraformaldehyde and stained by X-gal solution to visualize the graft-derived cells. Host embryos that contained positively stained graft-derived cells were then processed for histology and sectioned in paraffin wax. The number and the pattern of distribution of X-gal stained cells in the tissues of the host embryo were scored in serial sections of the specimen. Of the 142 host embryos in the transplantation experiments, 129 developed normally in culture and contained graft-derived cells and processed for histology, and 100 serially sectioned specimens were successfully analyzed for cell count and tissue distribution. Donor embryos that were cocultured with the host embryo were examined first to ascertain that they developed the abnormal head phenotype displayed by the null-mutant embryo in vivo. Samples of the extraembryonic tissues were then collected for genotyping by PCR analysis (Hukriede et al., 2003; Tsang et al., 2000), and the rest of the embryo was stained by X-gal reagent to confirm that the donor cells were transgenic for *Hmgcr–lacZ*.

Results

Regionalized tissue fates of the endodermal cells at late gastrulation

The developmental fates of the endodermal cells in the normal embryo were assessed by tracking the distribution of cells originating from different regions of the endoderm as the embryo developed from the no- to early bud stage to the early somite stage in vitro. As previously shown by Davidson et al. (2003), expression of the EGFP becomes detectable 2–3 h after electroporation with the CMV–EGFP expression vector (Fig. 2A) and thereafter for the duration of in vitro development (Fig. 2B). The distribution of the EGFP- and lacZ-expressing cells in embryos that were coelectroporated with two vectors was generally comparable (Figs. 2C and D). However, we have not determined whether the vectors were always coexpressed in the same cells. Nevertheless, this finding showed that the pattern of distribution of the electroporated cells is not influenced by the type of genetic marker. Histological examination of the specimen confirmed that the electroporation procedure specifically labeled the endodermal cells of the embryo (Fig. 2E).

In the E7.5 no- to early bud gastrula embryo, the boundary between the embryonic and extraembryonic

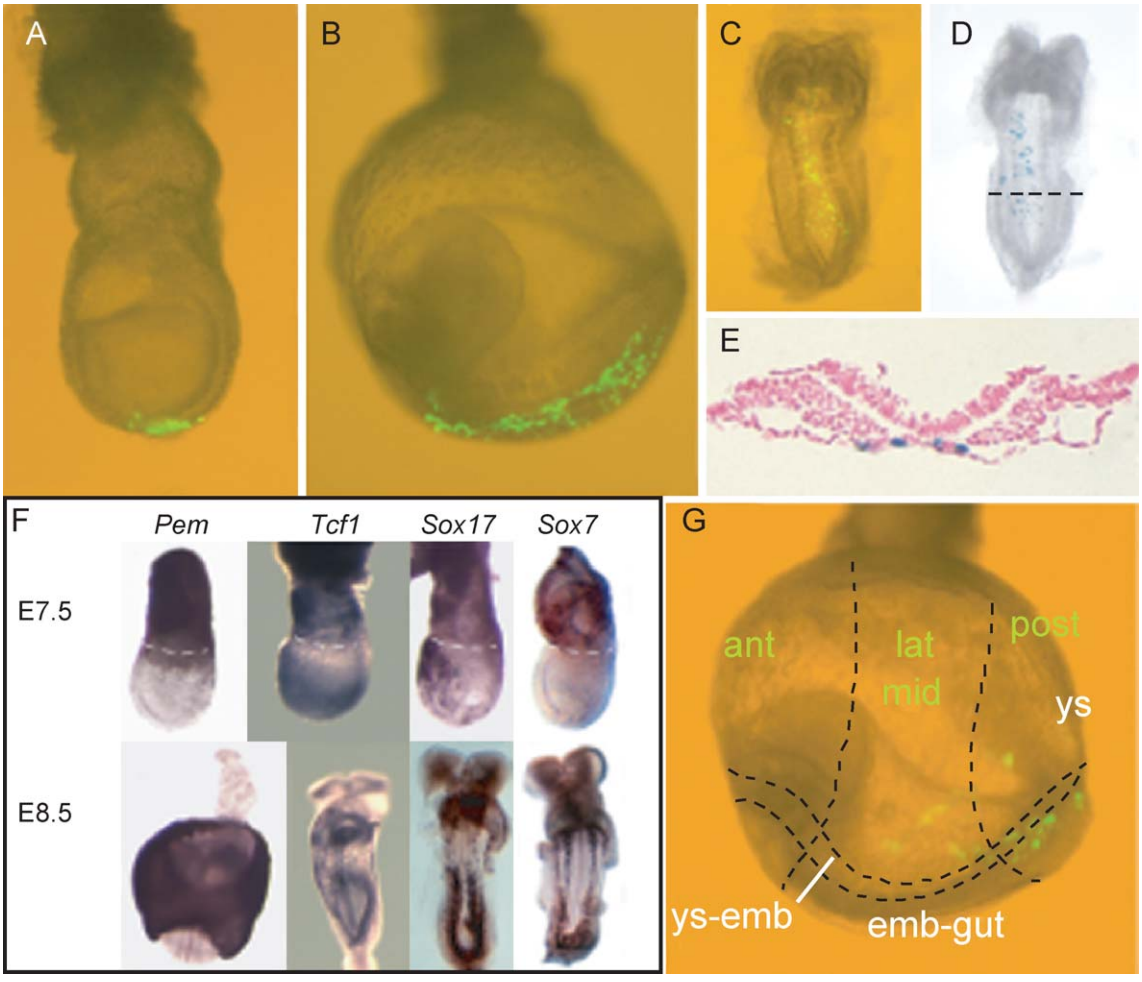

Fig. 2. (A) EGFP-expressing cells in an embryo 3 h after electroporation of the distal region with EGFP and *lacZ* expression vectors. (B–D) The same embryo after 24 h of in vitro development displaying the extensive distribution of the (B) EGFP-expressing cells along the anterior–posterior length of the embryonic gut and the similar pattern of distribution of the labeled cells revealed by the expression of (C) EGFP and (D) *lacZ* marker. (E) The labeled cells (blue X-gal stained cells) in the endodermal layer of the embryo (transverse section of the embryo at the level shown in D). (F) The expression pattern of *Pem*, *Tcf1/Hnf1*α, *Sox17*, and *Sox7* in the endoderm of E7.5 and E8.5 embryos. The white dashed lines mark the position of the amnion, which is the morphological landmark of the boundary between extraembryonic and embryonic part of the conceptus. In the E7.5 embryo, *Pem* is expressed in the extraembryonic endoderm and the endoderm in the proximal region of the embryo. *Tcf1* and *Sox7* are expressed in the endoderm proximal to the amnion. In the embryonic region, *Sox17* and *Tcf1* expression overlaps in the anterior distal region and *Tcf1* expression covers most of the embryonic domain except where *Pem* is expressed. In the E8.5 embryo, *Pem* is expressed in the yolk sac endoderm, *Tcf1*, and *Sox17* in the gut endoderm and *Sox7* in the vascular endothelium. (G) The scheme for scoring cells in the endoderm in the yolk sac (ys), yolk sac–embryo junction (ys–emb), and the embryonic gut (emb-gut), which are subdivided into anterior (ant), lateral (lat, for ys, and ys–emb), or middle (for emb-gut) and posterior (post) regions. This embryo contains 56 cells that are distributed in the yolk sac (lateral: 35%, posterior: 5%), yolk sac–embryo junction (lateral: 5%; posterior 20%), and embryonic gut (posterior: 35%).

domain of the conceptus can be discerned by the position of the amnion (white dashed line in Fig. 2F), which matches the distal border of the extraembryonic domain of *Tcf1/Hnf1α* and *Sox7* expression (Fig. 2F; E7.5). To map the fate of the endoderm in the embryonic compartment of the gastrula embryo, cells were labeled by targeting electroporation to one of the nine regions (Fig. 3A). Three of these regions are localized on the lateral aspect of the embryo. The anterior–lateral and the posterior–lateral sites are adjacent to the border of the embryonic and extra-embryonic parts of the conceptus. These two proximal regions contain endodermal cells that express *Pem*, which is also expressed by the endodermal cells in the extra-embryonic region (Fig. 2F; *Pem* E7.5), but not *Tcf1* (Fig. 2F; *Tcf1* E7.5). The lateral site occupies the lateral region of the embryo distal to the two proximal sites. The remaining six sites are located in the sagittal plane of embryo and they are in the anterior–posterior order, the anterior–proximal, anterior–distal, distal, posterior–distal, posterior–middle, and posterior–proximal sites. The anterior–proximal and the anterior–distal sites encompass the anterior axial and paraxial regions of the embryo, which overlap with *Sox17* expression domain (Fig. 2F; *Sox17* E7.5). The distal site contains the node and the endoderm at the distal tip of the embryo. The three posterior sites correspond to areas associated with the three respective segments of the primitive streak. All these sites except the three proximal sites are contained within the expression domain of *Tcf1* (Fig. 2F; *Tcf1* E7.5). When embryos were examined 3 h after electroporation, about 10–25 endodermal cells within an area of about 50–70 μm^2 were labeled in each embryo (Figs. 2A and 3B–J). The location of the labeled cells was generally consistent with the intended site of electroporation notwithstanding that during the 3-h period, labeled cells may have dispersed to some extent. After the location of the labeled cells was ascertained, embryos were cultured in vitro until the embryos reached the early (4–8) somite stage.

After 24 h of in vitro development, labeled cells were visualized by the expression of the fluorescent protein (Figs. 3B–J) and their number was scored on enhanced digital images of the embryo. The localization and the relative abundance of the descendants of the labeled population in the anterior, middle, and posterior regions of the yolk sac endoderm, the yolk sac embryo junction, and the prospective gut domain of the embryo were scored (Fig. 2G; Table 1). The anterior limit of the embryonic gut is taken as the edge of the ventral lip of the foregut invagination, whereas the yolk sac–embryo junction in other region of the embryo is demarcated by the meeting of the amnion, the yolk sac, and the lateral embryonic tissues. The yolk sac–embryonic endoderm junction (ys–emb; Fig. 2G) is also delineated by the juxtaposition of the expression domain of *Pem* (in the yolk sac endoderm; Fig. 2F, *Pem* E8.5) and *Tcf1* (in the gut endoderm; Fig. 2F, *Tcf1* E8.5) and *Sox17* (in the middle and posterior gut endoderm; Fig. 2F, *Sox17* E8.5).

Approximately 40–250 EGFP-expressing cells were found in the endoderm of the embryo of the nine sites of electroporation. Cells from each site were distributed in distinctive patterns to different parts of the yolk sac endoderm, the endoderm at the lateral region of the embryo adjacent to the yolk sac, and the prospective embryonic gut (Figs. 3B–J). Of specific interest is that the majority of labeled endodermal cells from the anterior–proximal, anterior–lateral, and posterior–lateral sites of the early bud embryos were allocated to the anterior and lateral yolk sac endoderm (Figs. 3B–D; Table 1). Cells from the anterior sites tended to be localized in the more anterior and lateral parts of the yolk sac while those from the lateral regions colonized mainly the lateral part of the yolk sac. The posterior yolk sac received relatively minor contribution from the posterior–lateral, posterior proximal, and posterior middle sites (Figs. 3D and E and data not shown; Table 1). These findings suggest that some "embryonic" endoderm in the proximal and lateral regions of the early bud embryo still display an extraembryonic fate. The presence of more labeled cells in the anterior and lateral regions of the yolk sac also suggests that the preexisting endoderm in the extraembryonic compartment may be displaced to the posterior yolk sac by the cells emigrating from the embryonic sites.

Contribution to endoderm along the yolk sac–embryo junction came from the proximal sites: anterior–proximal, anterior lateral, posterior–lateral, and posterior–proximal (Figs. 3B–E). In addition, descendants of endodermal cells at the more distal sites such as anterior–distal, lateral, and posterior–middle also colonized the yolk sac–embryo junction (Figs. 3H and I; Table 1). The lower propensity in the expansion of the posterior and lateral "embryonic" endoderm beyond the yolk sac–embryo junction is consistent with the concept that the proximal displacement of these cells is hindered by occupancy of the posterior part of the yolk sac by the resident extraembryonic cell population.

For analyzing the distribution of labeled cells in the embryonic gut, the number of EGFP-expressing cells localized in the foregut invagination (anterior gut) and in the endoderm underneath the paraxial and axial mesoderm in the middle and posterior region of the embryo was scored. Analysis of the distribution of labeled cells from the anterior proximal, anterior–lateral, and anterior–distal sites showed that all three regions contain progenitors of the yolk sac and foregut endoderm. The most preponderant contribution to the foregut endoderm was by cells in the anterior–distal and the distal sites. In contrast, cells in the anterior–proximal site tended to contribute more to the extraembryonic (anterior yolk sac) endoderm and less to the foregut endoderm than the more distal sites. Endoderm of the middle segment of the prospective gut of the early somite embryo was derived principally from the anterior–distal (Fig. 3F), distal (Fig. 3G), and posterior–distal sites (data not shown; Table 1). The posterior gut endoderm was colonized mainly by cells of the

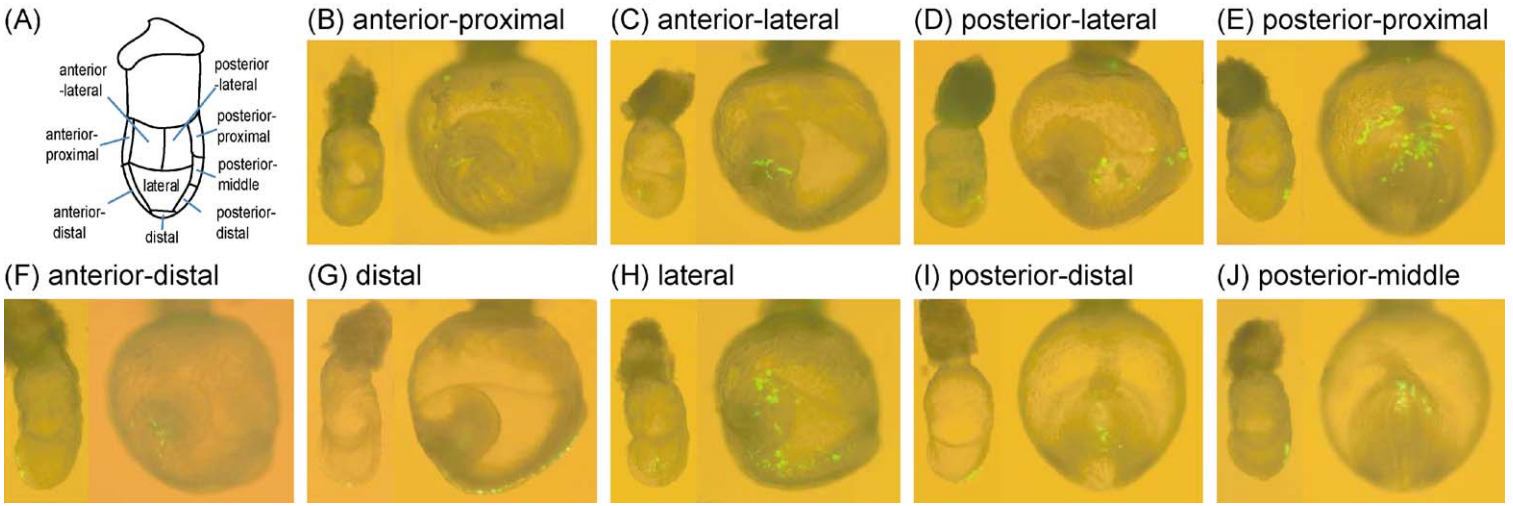

Fig. 3. Regionalization of cell fates in the endoderm of E7.5 early to late-bud stage *Lhx1+/+* and *Lhx1+/–* embryo. (A) The nine areas of the endoderm that were electroporated. (B–J) Examples of the distribution of the EGFP-expressing cells in the embryo visualized by fluorescence microscopy at 3 h (left-hand side) and 24 h (right-hand side) after electroporation (see Results and Table 1 for detail of the pattern of distribution). Lateral views of the embryo are shown with anterior of the embryo to the left, except for E, I, and J, which show the posterior view of embryo at the end of the experiment.

Table 1
Distribution of CMV–EGFP-labeled endodermal cells in *Lhx1*+/+ and *Lhx1*+/− embryos electroporated at the early bud stage and cultured for 24 h in vitro

Site of electroporation	No. embryos	Distribution of descendants of electroporated endodermal cells: percentage of total population								
		Yolk sac			Yolk sac–embryo junction			Embryonic gut		
		Anterior	Lateral	Posterior	Anterior	Lateral	Posterior	Anterior	Middle	Posterior
Anterior–proximal	6	55.0			26.7	5.0		13.3		
Anterior–lateral	4	51.2	17.5		18.8	7.5		5.0		
Posterior–lateral	3	16.7	48.3	6.7		3.3	8.3			16.7
Posterior–proximal	6		1.7	17.5			14.2		0.8	65.8
Anterior–distal	6	3.3			11.7	3.4		53.3	28.3	
Lateral	5	11	12		3	26	24		14	10
Posterior–middle	8		1.9	2.5			12.5			83.1
Distal	8							13.7	66.3	20.0
Posterior–distal	11						1.8	0.5	59.1	38.6

posterior–proximal, posterior–middle, and posterior–distal sites (Figs. 3E, I, and J), with a lesser contribution by cells in the distal, posterior–lateral, and lateral sites (Table 1).

Two morphogenetic patterns of the gut endoderm are worth special note. First, descendants of the endodermal cells at the distal site of the early bud embryo were spreading in almost the entire anterior–length of the embryonic gut (Fig. 3G; Table 1). These patterns of cell movement suggest that the morphogenesis of the embryonic gut is accomplished by the anterior–posterior extension of the endoderm in the length of the gut, which may be part of the convergence extension process associated with the elongation of the body axis. Second, the posterior–distal cell population appeared to extend posteriorly to occupy the medial area of the posterior gut (Fig. 3I), whereas the posterior–middle population was displaced posteriorly and laterally (Fig. 3J). The posterior–proximal population moved mainly laterally to the lateral areas of the posterior gut domain and spread anteriorly along the posterior yolk sac–embryo junction (Fig. 3E). These findings reveal a unique pattern of morphogenetic movement during the formation of the hindgut: the posterior extension of the endodermal cells underlying the anterior and middle segment of the primitive streak to the medial part of the posterior gut and the lateral displacement of the endoderm associated with posterior segment of the primitive streak to the lateral region of the posterior gut. The regionalization of the fates of the endoderm of the early bud embryo therefore not only heralds the allocation of progenitor cells for specific endodermal population but also provides an insight to the morphogenetic tissue movements that accompany the formation of the embryonic gut.

Loss of Lhx1 function is associated with abnormal endodermal fates

The *Lhx1*−/− embryos displayed a range of abnormal morphology at gastrulation, varying from severely malformed to moderate reduction in size and nearly normal shape (Figs. 1B, D, F, and H). Staging of the *Lhx1*−/− embryo by the standard morphological criteria was therefore not feasible. In this study, the developmental stage of the null-mutant embryos was taken to be comparable to that of the majority of the wild-type and heterozygous mutant littermates. Fate-mapping experiments were performed on null-mutant embryos of litters that consisted of morphologically normal no- to early bud embryos. The presence of a bulbous structure in the yolk sac cavity of the mutant embryo that resembles the allantoic bud (Figs. 1B and 4B–G) indicated that it would be reasonable to regard the mutant embryo as equivalent to no- to early bud stage. The allantoic budlike structure also pinpoints the posterior side of the embryo for the purpose of axis orientation. At the end of in vitro culture, the mutant genotype was affirmed by the abnormal development of the head folds and by PCR analysis of tissue sampled from selected specimens. The “mutant” morphology was not observed in the normal embryo in these experiments. Damages caused by electroporation or suboptimal embryo culture conditions led to severe and nonspecific abnormality and complete arrest of development.

The smaller size of the *Lhx1*−/− mutant embryo limited the number of sites that could be tested with practical level of precision. Endodermal cells in six sites were electroporated; five in the sagittal plane of the embryo: anterior–proximal, anterior–distal, distal, posterior–distal, and posterior–proximal; and one in the lateral region (Fig. 4A). Similar to the normal counterparts, endodermal cells in the three proximal sites colonized the anterior, lateral, and posterior yolk sac endoderm (Figs. 4B and C and data not shown; Table 2). Other descendants of the anterior–distal endoderm congregated to the yolk sac–embryo junction (Fig. 4E) and only 10% was in the poorly developed anterior region of the embryo (Table 2). Contribution to the endoderm at the yolk sac–embryo junction by cells of the proximal and the lateral sites in the mutant embryo (Table 2) was similar to those of equivalent sites in the normal embryo (Table 1). The unexpected results were the substantial contribution by the anterior–distal endoderm to the anterior yolk sac, the cells in the distal site to the lateral yolk sac and the yolk sac–embryo junction, and the posterior distal cells to the posterior yolk sac. The extraembryonic fate of the endodermal cells in these distal sites contrasts that of the equivalent population in the

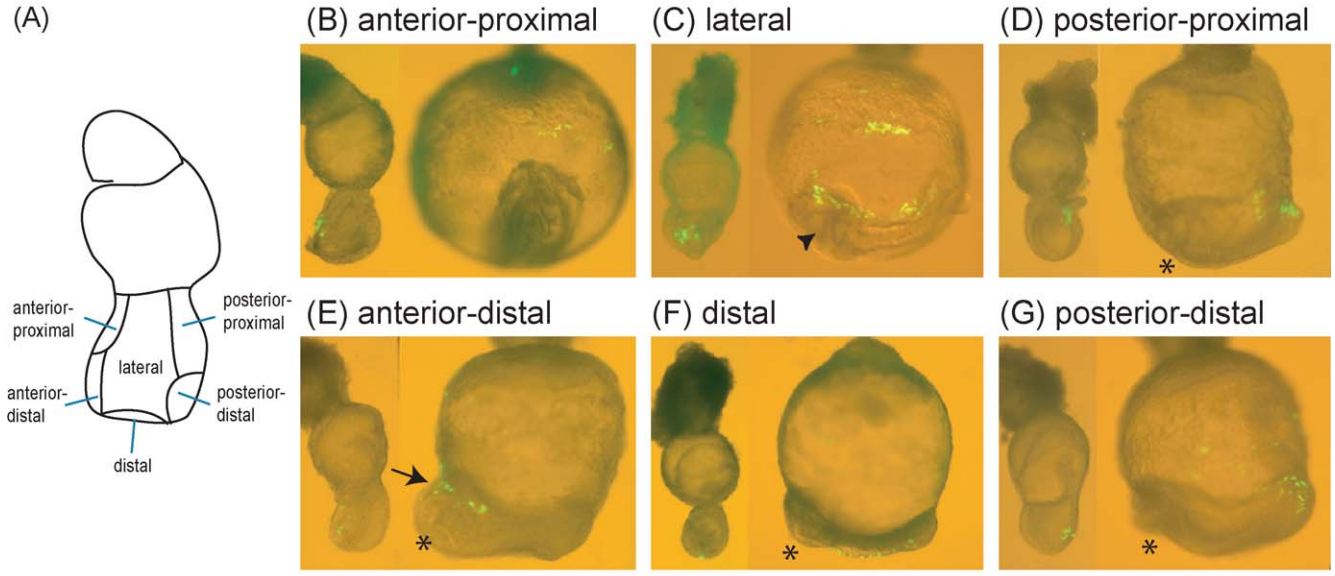

Fig. 4. Regionalization of cell fates in the endoderm of E7.5 *Lhx1−/−* embryos. (A) The six areas of the endoderm that were electroporated. (B–G) Examples of the localization of the EGFP-expressing cells in the embryo visualized by fluorescence microscopy at 3 h (left-hand side) and 24 h (right-hand side) after electroporation (see Results and Table 2 for detail of the pattern of distribution). Lateral views of the embryo are shown with anterior of the embryo to the left, except for B, which shows the anterior view of the embryo at the end of the experiment. The arrow in E indicates the yolk sac–embryo junction in the anterior region of the embryo. Foregut invagination is often absent (asterisk in D–G) in the *Lhx1−/−* mutant, though a rudimentary foregut portal may be formed in some embryos (arrowhead in C).

normal embryo (Table 1), suggesting progenitors of the extraembryonic endoderm are localized more distally in the anterior region of the mutant embryo. The contribution by the posterior–proximal and the posterior–distal sites to the posterior gut endoderm (Figs. 4D and G; Table 2) and the extensive anterior–posterior contribution of the distal site (Fig. 4F) were comparable to that of the normal counterpart. However, the overall contribution to the anterior gut endoderm by the anterior and distal sites and to the middle gut region by the posterior–distal site was reduced in the mutant embryo. There may be fewer gut progenitors in the endoderm at gastrulation and they are absent from the anterior region of the mutant embryo.

Loss of Lhx1 function does not affect the endodermal potency of epiblast cells

The loss of *Sox17* expression (Fig. 1D) and the reduction in the population of embryonic gut progenitors in the endoderm of the mutant embryo raise the question of whether the loss of *Lhx1* affects the allocation of the epiblast cells to the endodermal lineage. Cell transplantation experiments were performed to test if the endodermal potency of *Lhx1−/−* cells may be impaired. Previous embryological studies have shown that the progenitors of definitive (gut) endoderm are found in the posterior epiblast of early streak embryo (Lawson and Pedersen, 1987; Lawson et al., 1991; Tam et al., 1997) and in the germ layer tissues associated with the anterior segment of the primitive streak and the midgastrula organizer (Kinder et al., 2001b). Allocation of the definitive endoderm for the fore- and midgut begins at the early to midstreak stage (Lawson and Pedersen, 1987; Lawson et al., 1986; Tam and Beddington, 1992) and is mostly for the posterior gut by the late-streak to early bud stage (Beddington, 1981, 1982; Tam and Beddington, 1987). In view of these findings, lineage analysis experiments were performed using donor cells isolated from the mid- to late-streak stage embryo to ensure that the full potency of epiblast

Table 2
Distribution of CMV–EGFP-labeled endodermal cells in *Lhx1−/−* embryos electroporated at E7.5 and cultured for 24 h in vitro

Site of electroporation	No. embryos	Distribution of descendants of electroporated endodermal cells: percentage of total population								
		Yolk sac			Yolk sac–embryo junction			Embryonic gut		
		Anterior	Lateral	Posterior	Anterior	Lateral	Posterior	Anterior	Middle	Posterior
Anterior–proximal	6	80.0			18.0			2.0		
Lateral	14		50.0	1.4	2.1	29.3	10.0			7.1
Posterior–proximal	8		2.4	11.3		2.5	35.0			48.8
Anterior–distal	9	63.3			24.4	2.3		10.0		
Distal	9		8.8			4.4		24.4	35.5	26.7
Posterior–distal	10		2.0	3.0			7.0	3.0	16.0	69.0

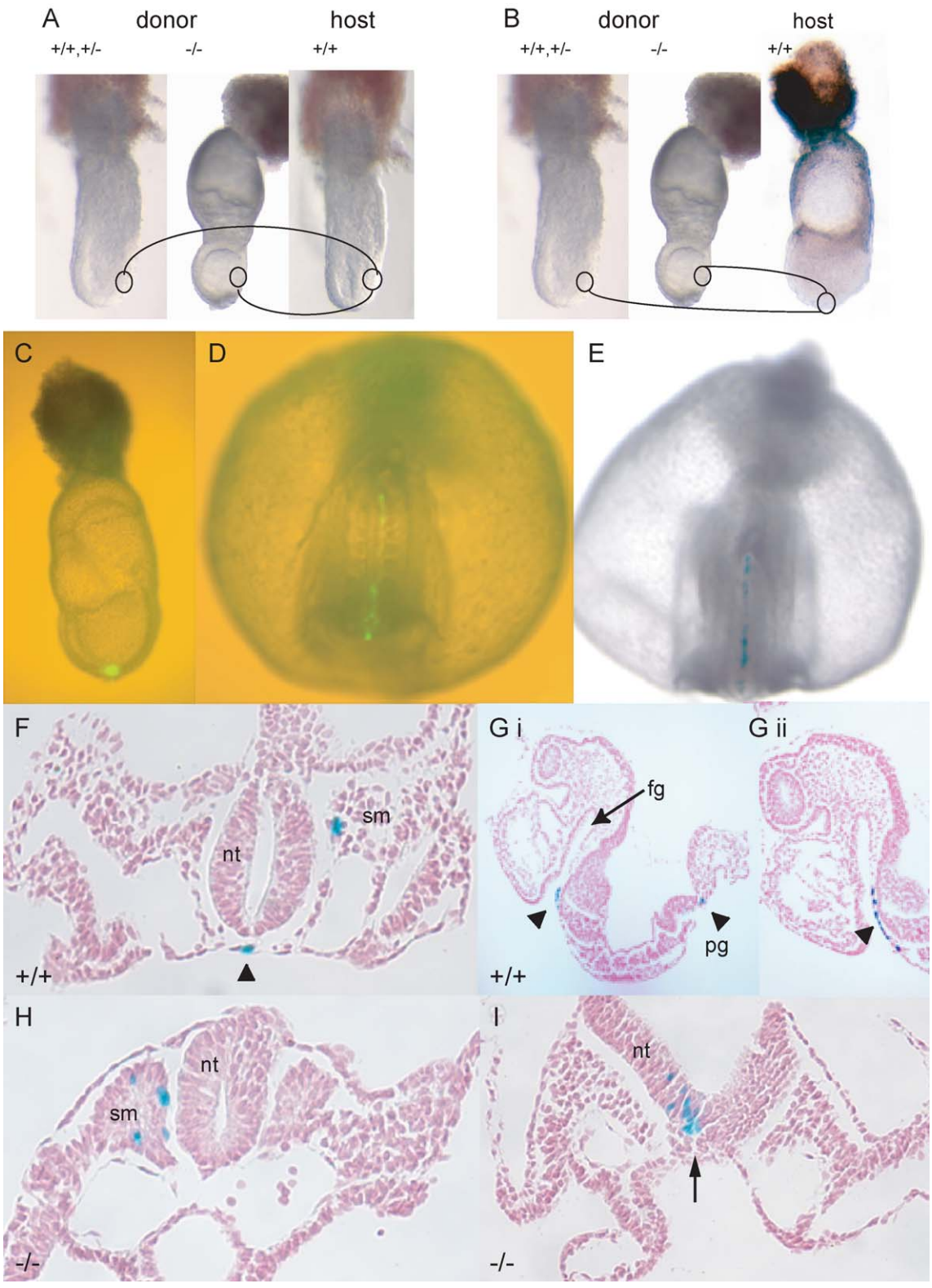

Fig. 5. (A and B) The experimental strategy for testing the lineage potency of cells in the anterior primitive streak of mid- to late-streak normal (+/+, +/−) embryo and in the posterior epiblast of mutant (−/−) embryo by transplantation to the anterior primitive streak of (A) midstreak or (B) no- to early bud host embryo. (C) Transplantation of wild-type EGFP and *lacZ*-transgenic donor cells to the node region of the early bud stage host embryo, resulting in the colonization of the axial mesoderm and endoderm of the host embryo after 24 h of in vitro development by graft-derived cells expressing (D) the EGFP and (E) the *lacZ* transgene (C–E are pictures of the same embryo). (F–I) Examples of presence of graft-derived *lacZ*-expressing cells [F and G: normal (+/+) cells; H and I: *Lhx1*−/− (−/−) mutant cells] in the somite (sm), notochord (arrowhead in F), endoderm (arrowheads in two different specimens: Gi and Gii) of the foregut (fg) and the posterior gut (pg), the neuroepithelium (nt), and the body of the primitive streak (arrow in I).

cells to contribute to endoderm of all gut regions could be tested by orthotopic and heterotopic transplantation (Figs. 5A and B). Litters of embryos from pregnant E7.0–E7.5 *Lhx1+/−;EGFP;Hmgcr–lacZ* mice were selected by the criterion that majority of the normal embryos was at the mid- to late-streak stage of gastrulation (Downs and Davies, 1993). Donor posterior epiblast cells were isolated from the anterior primitive streak of the normal embryo and from the middle to proximal regions of the posterior part of the mutant littermate (Figs. 5A and B), which encompass the *Foxa2* and *T* expression domain (Fig. 1F; Kinder et al., 2001a).

Donor cells from wild-type embryos were transplanted orthotopically to the anterior primitive streak of midstreak host embryo (Fig. 5A) and heterotopically and heterochronically to the node of no- to early bud host embryo (Figs. 5B and C). After 24–26 h of in vitro development, graft-derived cells in the host embryo were visualized by EGFP and *lacZ* expression (Figs. 5D and E). The number of graft-derived cells in the host embryo varied between the two types of transplantations. In the orthotopic type, 12–195 *lacZ*-positive cells were scored in the 22 host embryos, with a median of 73 and mean of 75.1 cells. The 16 host embryos receiving heterotopic transplantation contained more graft-derived cells: 36–244 cells with a median of 133 and a mean of 128.8. The data when viewed as a whole showed that the anterior primitive streak cells are able to contribute to all three germ layer derivatives in the host embryo. The number of graft-derived cells also varied between embryos receiving orthotopic or heterotopic transplantation. This may be due to the different number of cells grafted to the embryo and the fraction of this population that was incorporated and had produced viable cellular descendants in the host tissues. Cell death has been shown to occur regularly in the epiblast and the endoderm of the gastrula stage mouse embryo (Lawson et al., 1986; Poelmann, 1980, 1981). Neither the number of grafted cells nor cell viability could be controlled effectively and consistently in the transplantation experiment. Assuming that the variables (number of grafted cells and cell viability) were similar in both types of transplantation, the results showed that more graft-derived cells were found following transplanting the anterior primitive streak heterotopically to the node of the host embryo, which was also at a more advanced stage of development. The basis of this difference is not known.

Donor cells from the posterior epiblast of the mutant embryo were transplanted to the same two sites in the wild-type host embryo as for the normal donor cells (Figs. 5A and B). Host embryos with cells transplanted to the anterior primitive streak at midstreak stage contained between 10 and 407 cells with a median of 43 and a mean of 81.2 cells. The discrepancy between the median and the mean suggests that the number of graft-derived cells in these host embryos did not conform to a normal statistical distribution and the majority of the host embryos have a lower graft-derived cell number than the arithmetic mean. Like the normal counterpart, the transplantation to the node resulted in the presence of more graft-derived cells in the host embryo: between 10 and 511 cells with a median of 123 and a mean of 156.5. The two data sets when considered together as a test of the overall lineage potency of the *Lhx1−/−* mutant cells showed no evidence of any restriction of lineage potency (Table 3). A noticeable departure from the normal cells, however, is the less prolific contribution of the mutant cells in the endoderm after transplantation to the anterior primitive streak of the midstreak stage host embryo, but not so when transplanted to the node of no- to early bud host embryo (Table 3). Nevertheless, contribution to the endodermal population was evident irrespective of the site of transplantation indicating that loss of *Lhx1* function does not impact significantly on the endodermal potency of the epiblast cells.

The overall patterns of tissue contribution by the normal or mutant cells were similar for the two types of transplantations. Graft-derived cells were found in derivatives of all three germ layers (e.g., Figs. 5F–I: notochord, somite, and gut endoderm; Table 3 and histological data not shown). A major difference between the two types of transplantation was the presence of the donor cells in the heart mesoderm when they are transplanted to the midstreak stage and the greater contribution to the paraxial mesoderm when they are transplanted to the node (Table 3). This is probably related to the timing of most active allocation of heart mesoderm and the paraxial mesoderm at the midstreak stage and at the no- to early bud stage, respectively (Beddington, 1981; Lawson et al., 1991; Tam and Beddington, 1987; Tam et al., 1997).

Of specific note is the overrepresentation of graft-derived mutant cells in the posterior mesoderm and the primitive streak of the host embryo (Figs. 5H and I; Table 3). This finding is consistent to the previous result of cell transplantation that the mutant cells tend to remain in the primitive streak and are less able to participate in the anterior morphogenetic movement of mesoderm after incorporation into the paraxial mesoderm (Hukriede et al., 2003) or the lateral plate mesoderm (Tsang et al., 2000). In contrast, the presence of mutant cells in the foregut of the host embryo suggests that morphogenetic movement of the endodermal cells is unaffected by the loss of *Lhx1* function. This may suggest that the lack of the gut endoderm progenitor in the anterior region of the null-mutant embryo might be either due to the failure of anterior morphogenesis, which prohibits any anterior movement of the endodermal progenitors or that the movement of the endoderm is impeded secondarily due to the defects in the migration of the paraxial mesoderm or the axial mesoderm (Hukriede et al., 2003).

To test the latter possibility, whole tissue fragments isolated from the midgastrula organizer of normal midstreak embryos, the node of normal early bud embryo, and the posterior epiblast of the *Lhx1−/−* embryos were transplanted to the lateral site of the no- to early bud stage host embryo (Fig. 6A; Beddington, 1994; Tam and Steiner,

Table 3
The distribution of graft-derived cells in the tissues of host embryo following transplantation of EGFP and *lacZ*-expressing posterior epiblast cells of *Lhx*+/+, *Lhx*+/−, and *Lhx1*−/− embryos to nontransgenic wild-type host embryos and cultured for 24 h in vitro

Donor genotype and tissue	*Lhx1*+/+ or *Lhx1*+/−		*Lhx1*−/−	
	Anterior primitive streak: mid-streak stage		Posterior epiblast	
Site of grafting: sage of host embryo	Orthotopic Anterior primitive streak: mid-streak	Heterotopic Anterior primitive streak/node: no- to early bud	Anterior primitive streak: mid-streak	Anterior primitive streak/node: no- to early bud
No. analyzed	22 hosts (8 donors)	16 hosts (9 donors)	35 hosts (11 donors)	27 hosts (8 donors)
Mean cell number/embryo (total; median: range)	75.1 ± 12.4 (1648; 73: 12–195)	128.8 ± 16.9 (2061; 133: 36–244)	81.2 ± 14.4 (2843; 43: 10–407)	156.5 ± 24.0 (4069; 123: 10–511)
Tissue contribution: number of cells (number of embryos) and percentage of total graft-derived population				
Gut endoderm				
Foregut	40(6) 2.4%	112(5) 5.4%	51(4) <2%	108(12) 2.7%
Midgut	187(9) 11.3%	76(9) 3.7%	48(10) <2%	136(11) 3.3%
Hindgut	59(2) 3.6%	21(4) <2%	10(2) <2%	102(5) 2.5%
Axial mesoderm				
Head process	17(3) <2%	0	22(1) <2%	44(4) <2%
Notochord	61(6) 3.7%	267(9) 12.9%	115(14) 4.0%	200(16) 4.9%
Floor plate				
Brain	0	20(4) <2%	4(1) <2%	429(12) 10.5%
Spinal cord	19(1) <2%	71(5) 3.4%	95(10) 3.3%	153(10) 3.8%
Neuroepithelium				
Brain	0	14(3) <2%	58(3) 2%	359(8) 8.8%
Spinal cord	6(2) <2%	251(7) 12.2%	148(8) 5.2%	103(5) 2.5%
Paraxial mesoderm				
Cranial mesenchyme	426(11) 25.8%	754(12) 36.5%	795(17) 27.9%	823(15) 20.2%
Somite	495(17) 30.0%	378(9) 18.3%	907(16) 31.9%	587(9) 14.4%
Presomitic	17(1) <2%	68(4) 3.3%	143(4) 5.0%	566(5) 13.9%
Posterior/primitive streak	70(3) 4.3%	25(1) <2%	248(5) 8.7%	426(5) 10.4%
Lateral mesoderm	56(4) 3.4%	4(1) <2%	82(1) 2.9%	4(1) <2%
Heart	195(4) 11.8%	0	117(1) 4.1%	29(1) <2%

1999). The ability of the graft to undergo convergence extension that is characteristic of the morphogenetic behavior of the derivatives of the gastrula organizer such as axial mesoderm (notochord) and the floor plate was examined after 24 h of in vitro development (Figs. 6B–D). The result of this experiment showed that *Lhx1*−/− tissues

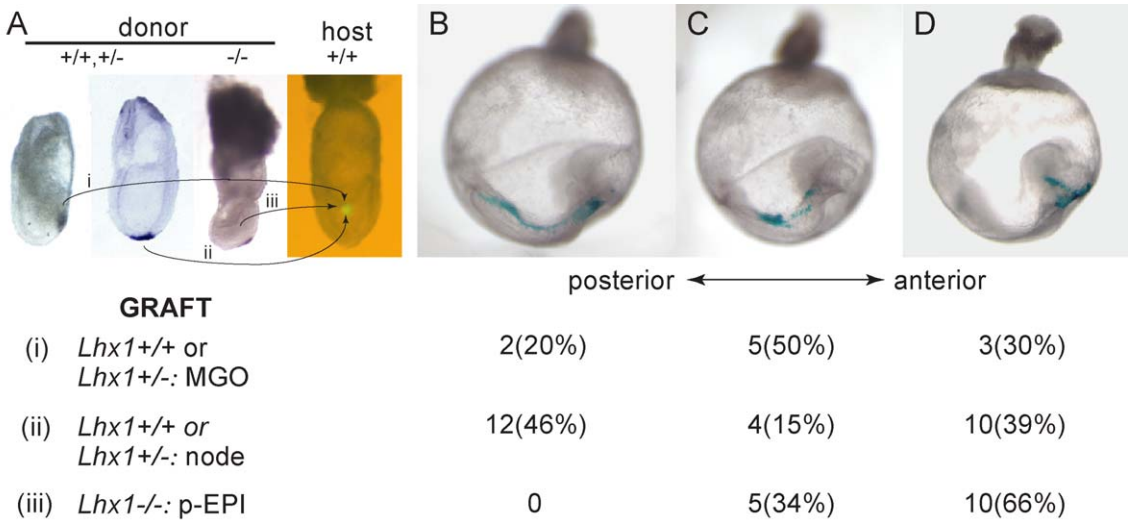

Fig. 6. (A) Transplantation of the *Chrd*-expressing tissue of the midgastrula organizer, the node (*Lhx1*+/+, +/−), or the posterior epiblast (*Lhx1*−/−) to the lateral region of an early bud stage wild-type host embryo (the graft is revealed by the expression of the EGFP transgene). (B–D) The morphogenetic behavior of the transplanted tissues: (B) tissue extended in a tight column along the anterior–posterior axis in the lateral (right flank) region of the host embryo, (C) tissue extended and dispersed in the host tissues, and (D) tissue incorporated into the host tissues locally and not extended. The tabulated data show the number and relative frequency (%) of grafts displaying the three categories (B–D) of morphogenetic behavior in the host embryo. MGO, midgastrula organizer; p-EPI, posterior epiblast.

were less capable of undergoing convergence extension in the wild-type host than the normal counterpart (Fig. 6; tabulated data). The defective extension of the axial tissues may be a possible cause of the overall inefficient deployment of embryonic tissues including the endoderm to the anterior region of the mutant embryo.

Discussion

Regionalization of cell fates in the endoderm reveals a blueprint of the embryonic gut

In the present study, fate-mapping experiments were performed by tracking the origin and movement of the endodermal cells of the early bud stage mouse embryo. Similar analysis of endodermal cell fate has been accomplished for the neural plate/late-streak stage mouse embryo, in which clones of single cells were marked by iontophoretic injection of horseradish peroxidase and the clonal descendants were identified at the conclusion of the experiment by histochemical enzyme reaction (Lawson et al., 1986). This experimental approach is particularly robust for assessing the pluripotency and the population growth of endodermal cells. In contrast, our study employed the electroporation technique to introduce the CMV–EGFP and *Hmgcr–lacZ* expression vector into groups of endodermal cells to enable their descendants be traced by the expression of the fluorescence protein in a noninvasive and real-time manner. In addition, the fates of cells originating from nine sites covering the entire population of endoderm in the embryonic compartment of the late-gastrulation mouse conceptus were assessed. Our findings have therefore complemented and extended those of the previous analysis, which was focussed on the axial endoderm of the mouse gastrula.

Despite the differences in the experimental design and technique, developmental fates of endodermal cells revealed in the this study and that of Lawson et al. (1986) are remarkably concordant, specifically of those in the axial (sagittal) region of the early bud stage embryo (anterior–proximal, anterior–distal, distal, and posterior–distal; Figs. 3A and 7Ai of the present study, which are equivalent to regions I, II, III, and IV; Fig. 8b of Lawson et al., 1986). Descendants of cells in the anterior–proximal (I) and anterior–distal sites (II) colonize the endoderm of both the yolk sac and the foregut endoderm (Figs. 7Aii and iii). Cells in the more proximal zone contribute more substantially to the extraembryonic endoderm than those located more distally (Fig. 7Ai). Analyses of cell fate of the endoderm

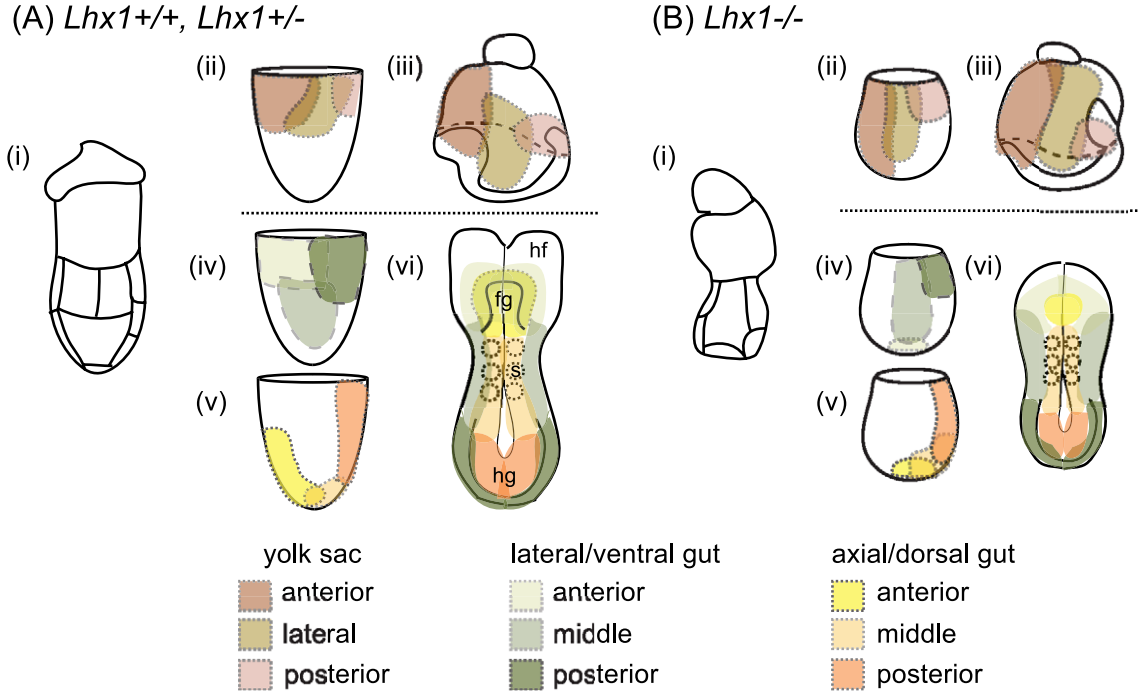

Fig. 7. Fate-maps of the endoderm of (A) no- to early bud stage *Lhx1+/+* and *Lhx1+/−* embryo and (B) *Lhx1−/−* mutant E7.5 embryo. (i) The areas of the endoderm fate-mapped by electroporation with the *EGFP* expression vector. (ii and iii) Lateral view of the endoderm showing the domains of progenitor cells of anterior, lateral, and posterior yolk sac endoderm at the (ii) no- to early bud stage and (iii) early somite stage. (iv and v) Lateral view of the endoderm showing the domains of progenitor cells of the endoderm of the (iv) lateral gut endoderm and (v) the axial gut endoderm. (vi) Ventral view of the early somite stage embryo showing the distribution of the progenitor population in the endoderm of the no- to early bud embryo to the yolk sac–embryo junction corresponding to the lateral region of the open gut, which later become the lateral and the ventral wall of the gut tube, and to the axial and paraxial areas of the gut which form the dorsal and the dorsolateral wall of the gut tube. The various populations of extraembryonic and embryonic endoderm are color coded. Overlapping domains of progenitors in maps ii to iv are highlighted by the change in shade where the colors merge. The mutant embryo (Bvi) generally lacks foregut invagination and forms a small and abnormal head fold. Abbreviations (Avi): hf, head folds; fg, foregut; hg, hind (posterior) gut; s, somite.

at the equivalent sites of the embryo at earlier stages of gastrulation revealed that anterior endoderm of the pre- and early streak stage embryo is fated primarily for extraembryonic endoderm, and by the midstreak stage there is increasing presence of cells in these anterior sites that will contribute progeny to the foregut endoderm (Lawson and Pedersen, 1987; Lawson et al., 1986). By tracking the distribution of descendants of cells already resident and those that were recruited from the epiblast to the endoderm in the posterior region of the midstreak embryo (Lawson et al., 1986; Tam and Beddington, 1992), it was revealed that there is progressive expansion of the definitive (gut) endoderm from the posterior to the anterior regions of the embryo during gastrulation. This would lead to the displacement the anterior endodermal population to extraembryonic sites by the incoming definitive endoderm. However, the resident anterior endoderm is not completely replaced by the immigrant cells since about 90% of the anterior–proximal and anterior–distal endodermal population of the late-streak embryo is made up of cells derived from the epiblast and the remaining 10% is derived from the preexisting visceral endoderm (Tam and Beddington, 1992). This may account for the presence of progenitors of both extraembryonic and foregut (lateral and medial) endoderm in the anterior region of the early bud embryo (Figs. 7Aii, iv, and v) and that the exit of cells to the extraembryonic endoderm will continue past the early bud stage (Lawson et al., 1986; Shimono and Behringer, 2003; and this study). The expression of molecular markers such as *Pem* and *Tcf1* suggests that endodermal cells in the proximal region of the embryonic domain are molecularly different from the more distal localized gut endoderm. Despite this apparent distinction in genetic activity, it is still unclear whether the endoderm that contribute to the yolk sac are descendants of the preexisting visceral endoderm that occupies the proximal boundary of the epiblast or the definitive endodermal cells that also contribute to the gut endoderm. A novel finding of the present study is that the colonization of different parts of the yolk sac by cells derived from the embryonic sites is not uniform. EGFP-expressing cells originating from the proximal "embryonic" domains were found mostly in the anterior and lateral regions and less in the posterior region of the yolk sac (Figs. 7Aii, iii). This may suggest that during postgastrulation development, endodermal cells move from the anterior and lateral "embryonic" sites to the extraembryonic compartment to occupy the anterior and lateral regions of the yolk sac while the posterior part of the yolk sac is populated mainly by the extraembryonic endoderm preexisting at the early bud stage of development.

Cells of the embryonic gut are derived from multiple sites in the endoderm of the early bud stage embryo. Progenitors of the endoderm of the anterior gut are found primarily in the anterior region and the distal site, those of middle and posterior parts of the gut are localized in the distal and posterior–distal sites (Fig. 7Av; regions II, III and IV of Lawson et al., 1986). Two other sites in the sagittal plane that have not been previously examined were found to contribute cells to the embryonic gut: the posterior–middle and the posterior–proximal sites contain progenitors of the posterior gut endoderm (Figs. 7Av and vi). The distribution of the EGFP-expressing cells in the gut of the early somite stage embryo (Fig. 7Avi) reveals site-specific patterns of cell movement that accompanies gut formation. Cells from the distal site (containing the endoderm and the node) are distributed in the axial and paraxial regions to all anterior–posterior levels of the gut. The extended distribution of the endoderm may accompany (or be driven by) the morphogenetic extension of the axial mesendoderm of the node and the head process (Beddington, 1994; Kinder et al., 2001b; Lawson et al., 1986). In contrast, cells from the neighboring posterior–distal site (underneath the anterior segment of the primitive streak) are distributed mainly to the axial area of the middle and posterior segments of the gut (see also Lawson et al., 1986). Cells from the posterior middle site (underneath the middle segment of the primitive streak) move to the axial region in the posterior-most domain of the gut as well as to the lateral region of the embryonic gut. Cells from the posterior–proximal region spread laterally and anteriorly to occupy the lateral region of the posterior gut (Figs. 7Av and vi). Therefore, the anterior–posterior position of the endodermal progenitor along the length of the primitive streak correlates with the mediolateral destination of their descendant in the posterior segment of the gut. This finding in the mouse is consistent with the concept of the translation of rostrocaudal position of the endodermal progenitors in the primitive streak to the mediolateral position in the gut during avian gastrulation (Lawson and Schoenwolf, 2003).

The origin of the endoderm in the lateral part of the embryonic gut was examined in our fate-mapping experiment of the early bud stage mouse embryo. Cells from all the proximal sites (i.e., anterior–proximal, anterior–lateral, posterior–lateral, and posterior–proximal) all contribute to the endoderm localized over the junction of the yolk sac and the embryonic gut domain (Figs. 7Aiv and vi). Additional contribution is provided by cells in the anterior–distal, lateral, and posterior–distal sites that occupy the middle third region along the proximal–distal axis of the embryo, with the lateral site being the major source of the lateral gut endoderm (Fig. 7Aiv). In the anterior region, endoderm in this junctional zone is likely to become the endoderm lining the ventral part of the foregut (Kirby et al., 2003), while those in the middle and posterior regions may form the lining of the lateral wall and floor of the midgut and the hindgut following the closure of the gut tube.

Lhx1 function is required for positioning the anterior gut endoderm

The finding that down-regulation of *XLim1* activity in the *Xenopus* mesodermal cells may impair their ability to

separate from the animal cap tissues (Hukriede et al., 2003) points to the possibility that loss of *Lhx1* function may impact on the allocation of the endoderm from the mesendodermal progenitors in the primitive streak of the mouse embryo, which might lead to the deficiency of definitive endoderm. Testing lineage potency of the *Lhx1*-deficient posterior epiblast cells by cell transplantation revealed that *Lhx1* function is not essential for the allocation of cells to the endodermal tissues—a finding that concurs with the outcome of chimera analysis (Shawlot et al., 1999). The lack of *Sox17* activity in the *Lhx1−/−* embryo suggests that the mutant endodermal cells may be unable to differentiate properly or to remain proliferative and viable (Kanai-Azuma et al., 2002). *Lhx1* activity is expressed primarily in the mesoderm and the visceral endoderm and not in the definitive endoderm (Shawlot and Behringer, 1995; Shawlot et al., 1999), and there are presently no data suggesting that *Lhx1* activity in the mesoderm is involved with signaling to the endoderm. To test more stringently the differentiation potency of the *Lhx1−/−* endodermal cells in the chimera obtained by introducing embryonic stem cells into the blastocyst or transplantation of cells into postimplantation embryos would require the assay of a robust reporter of cell differentiation that could be expressed specifically in the mutant cells (see Tsang et al., 2000). Alternatively, the impact on endoderm allocation and differentiation may be studied by tissue-specific ablation of *Lhx1* activity by conditional mutation. The animal resources and the molecular tools for either investigation are presently not available. Until these experiments can be done, it remains unclear whether or not *Lhx1* function is required for endodermal differentiation.

Fate-mapping study of the mutant embryo has revealed that the regionalization of the endodermal progenitors of the embryonic gut is abnormal and the movement of cells in the endoderm may be impeded. Cells fated for the embryonic gut are absent from the anterior endoderm of the *Lhx1−/−* embryo (Figs. 7Biv, v, and vi), which contains predominantly the progenitors of anterior yolk sac endoderm (Figs. 7Bii and iii). The majority of the progenitors of anterior gut endoderm are sequestered to the posterior and distal region of the endoderm while those of the other segments of the gut are found at sites equivalent to those in the normal embryo (Figs. 7Bv and vi). The abnormal regionalization of the progenitors of anterior definitive endoderm and the ectopic expression domain of primitive streak and gastrula organizer genes (Kinder et al., 2001b) suggest that embryonic patterning is defective in the absence of *Lhx1* activity. During the pregastrulation development of the mouse, cells in the visceral endoderm (VE) are displaced from the distal to the prospective anterior region of the prestreak embryo. This unique pattern of cell movement results in the realignment of the anterior–posterior (A–P) polarity of the endoderm tissues to the future A–P axis of the embryo (Beddington and Robertson, 1999; Thomas and Beddington, 1996). Active migration of cells may account for the displacement of cells from the distal to the prospective anterior region of the visceral endoderm (Srinivas et al., 2004). In addition, cells in the visceral endoderm may also be mobilized by the propulsive force generated by differential rate of cell proliferation under the influence of nodal signaling activity (Yamamoto et al., 2004). In the light that *Otx2* may interact with *Lhx1* in regulating nodal signaling (Perea-Gomez et al., 2001), a possible link between the activity of LIM domain protein activity and Nodal signaling has been postulated based on the impediment to the movement of the visceral endoderm following the loss of *Otx2* function (Suda et al., 1999).

Defects in cell movement have been associated with the loss or reduction of *Lhx1* activity during gastrulation. When *Lim1/Lhx1* activity is suppressed in the *Xenopus* embryo, anterior–posterior extension of the axial mesendoderm is disrupted due to the lack of PAPC activity (Hukriede et al., 2003). In the mouse, *Lhx1−/−* cells are sequestered to the posterior region of the paraxial mesoderm and lateral mesoderm and in the body of the primitive streak during gastrulation (Hukriede et al., 2003; Tsang et al., 2000; this study), and the *Lhx1*-deficient posterior epiblast fails to display morphogenetic behavior that may be related to the convergence extension of the mesendodermal derivatives of the gastrula organizer (this study). Loss of *Lhx1* activity has been shown to be accompanied by the down-regulation of angiomotin (Shimono and Behringer, 1999), which is essential for the exit of the anterior endodermal cells from the embryonic compartment to the yolk sac and the lateral movement of the anterior endoderm of the late-streak stage embryo (Shimono and Behringer, 2003). A likely cause of the deficiency of definitive endoderm in the anterior region of the *Lhx1−/−* gastrula embryo may be either due to the delayed development of the mutant embryo such that the endoderm destined for extraembryonic fate still remains in the anterior and distal region of the embryo. Alternatively, the sequestration of the definitive (gut) endoderm to the posterior regions is caused by the inefficient movement of the anterior definitive endoderm due to the blockage imposed by the prolonged retention of the visceral endoderm in the anterior region of the embryo and the defective morphogenetic movement of the axial mesendoderm and the paraxial mesoderm. The axial mesendoderm and the anterior definitive (gut) endoderm have been shown to play an essential role in the induction of anterior neural tissues and the morphogenesis of head structures (Bachiller et al., 2000; Camus et al., 2000; Martinez Barbera et al., 2000; Petryk et al., 2004; Stottmann et al., 2004; Zakin and De Robertis, 2004). As the data stand, the impact of loss of *Lhx1* function is more likely on the gastrulation movement of cells such as the segregation of the mesoderm and endoderm from other primitive streak cells (Hukriede et al., 2003) and the impaired morphogenetic movement of the severely depleted population of mesodermal (Hukriede et al., 2003) and endodermal (this study) cells in the mutant embryo. The failure to move the visceral endoderm and to

deploy the anterior definitive endoderm to the appropriate position during gastrulation and the lack of functionally competent definitive endoderm may underpin the defective morphogenesis of head structures caused by the loss of *Lhx1* function.

Acknowledgments

We thank Miles Wilkinson, Jacqueline Barra, and Janet Rossant for the gift of riboprobes and Samara Lewis and Peter Rowe for comments on the manuscript. Our work is supported by the Human Frontier Science Program (project grant to RRB, PPLT, S.-L. Ang, and H. Sasaki), the Ramaciotti Foundation, the National Health and Medical Research Council (NHMRC) of Australia, and Mr. James Fairfax. PPLT is an NHMRC Senior Principal Research Fellow.

References

Ang, S.L., Rossant, J., 1993. Anterior mesendoderm induces mouse Engrailed genes in explant cultures. Development 118, 139–149.

Bachiller, D., Klingensmith, J., Kemp, C., Belo, J.A., Anderson, R.M., May, S.R., McMahon, J.A., McMahon, A.P., Harland, R.M., Rossant, J., De Robertis, E.M., 2000. The organizer factors Chordin and Noggin are required for mouse forebrain development. Nature 403, 658–661.

Beddington, R.S.P., 1981. An autoradiograpic analysis of the potency of embryonic ectoderm in the 8th day postimplantation mouse embryo. J. Embryol. Exp. Morphol. 64, 87–104.

Beddington, R.S.P., 1982. An autoradiographic analysis of tissue potency in different regions of the embryonic ectoderm during gastrulation in the mouse. J. Embryol. Exp. Morphol. 69, 265–285.

Beddington, R.S.P., 1994. Induction of a second neural axis by the mouse node. Development 120, 613–620.

Beddington, R.S.P., Robertson, E.J., 1999. Axis development and early asymmetry in mammals. Cell 96, 195–209.

Camus, A., Tam, P.P.L., 1999. The organizer of the gastrulating mouse embryo. Curr. Top. Dev. Biol. 45, 117–153.

Camus, A., Davidson, B.P., Billiards, S., Khoo, P.L., Rivera-Perez, J.A., Wakamiya, M., Behringer, R.R., Tam, P.P.L., 2000. The morphogenetic role of midline mesendoderm and ectoderm in the development of the forebrain and the midbrain of the mouse embryo. Development 127, 1799–1813.

Chen, A.F., Behringer, R.R., 1995. Twist is required in head mesenchyme for cranial neural tube morphogenesis. Genes Dev. 15, 686–699.

Davidson, B.P., Tsang, T.E., Khoo, P.L., Gad, J.M., Tam, P.P.L., 2003. Introduction of cell markers into germ layer tissues of the mouse gastrula by whole embryo electroporation. Genesis 35, 57–62.

de Souza, F.S., Niehrs, C., 2000. Anterior endoderm and head induction in early vertebrate embryos. Cell Tissue Res. 300, 207–217.

Downs, K.M., Davies, T., 1993. Staging of gastrulating mouse embryos by morphological landmarks in the dissecting microscope. Development 118, 1255–1266.

Hadjantonakis, A.K., Gertsenstein, M., Ikawa, M., Okabe, M., Nagy, A., 1998. Generating green fluorescent mice by germline transmission of green fluorescent ES cells. Mech. Dev. 76, 79–90.

Hukriede, N.A., Tsang, T.E., Habas, R., Khoo, P.L., Steiner, K., Weeks, D.L., Tam, P.P.L., Dawid, I.B., 2003. Conserved requirement of Lim1 function for cell movements during gastrulation. Dev. Cell 4, 83–94.

Kanai-Azuma, M., Kanai, Y., Gad, J.M., Tajima, Y., Taya, C., Kurohmaru, M., Sanai, Y., Yonekawa, H., Yazaki, K., Tam, P.P.L., Hayashi, Y., 2002. Depletion of definitive gut endoderm in Sox17-null mutant mice. Development 129, 2367–2379.

Kinder, S.J., Tsang, T.E., Ang, S.-L., Behringer, R.R., Tam, P.P.L., 2001a. Defects of the body plan of mutant embryos lacking *Lhx1*, *Otx2* or *Hnf3β* activity. Int. J. Dev. Biol. 45, 347–355.

Kinder, S.J., Tsang, T.E., Wakamiya, M., Sasaki, H., Behringer, R.R., Nagy, A., Tam, P.P.L., 2001b. The organizer of mouse gastrula is composed of a dynamic population of progenitor cells for the axial mesoderm. Development 128, 3623–3634.

Kirby, M.L., Lawson, A., Stadt, H.A., Kumiski, D.H., Wallis, K.T., McCraney, E., Waldo, K.L., Li, Y.X., Schoenwolf, G.C., 2003. Hensen's node gives rise to the ventral midline of the foregut: implications for organizing head and heart development. Dev. Biol. 253, 175–188.

Lawson, K.A., Pedersen, R.A., 1987. Cell fate, morphogenetic movement and population kinetics of embryonic endoderm at the time of germ layer formation in the mouse. Development 101, 627–652.

Lawson, A., Schoenwolf, G.C., 2003. Epiblast and primitive-streak origins of the endoderm in the gastrulating chick embryo. Development 130, 3491–3501.

Lawson, K.A., Meneses, J.J., Pedersen, R.A., 1986. Cell fate and cell lineage in the endoderm of the presomite mouse embryo, studied with an intracellular tracer. Dev. Biol. 115, 325–339.

Lawson, K.A., Meneses, J.J., Pedersen, R.A., 1991. Clonal analysis of epiblast fate during germ layer formation in the mouse embryo. Development 113, 891–911.

Martinez Barbera, J.P., Clements, M., Thomas, P., Rodriguez, T., Meloy, D., Kioussis, D., Beddington, R.S.P., 2000. The homeobox gene Hex is required in definitive endodermal tissues for normal forebrain, liver and thyroid formation. Development 127, 2433–2445.

Perea-Gomez, A., Rhinn, M., Ang, S.L., 2001. Role of the anterior visceral endoderm in restricting posterior signals in the mouse embryo. Int. J. Dev. Biol. 45, 311–320.

Petryk, A., Anderson, R.M., Jarcho, M.P., Leaf, I., Carlson, C.S., Klingensmith, J., Shawlot, W., O'Connor, M.B., 2004. The mammalian twisted gastrulation gene functions in foregut and craniofacial development. Dev. Biol. 267, 374–386.

Poelmann, R.E., 1980. Differential mitosis and degeneration patterns in relation to the alterations in the shape of the embryonic ectoderm of early post-implantation mouse embryos. J. Embryol. Exp. Morphol. 55, 33–51.

Poelmann, R.E., 1981. The head-process and the formation of the definitive endoderm in the mouse embryo. Anat. Embryol. 162, 41–49.

Shawlot, W., Behringer, R.R., 1995. Requirement for *Lim1* in head organiser function. Nature 374, 425–430.

Shawlot, W., Wakamiya, M., Kwan, K.M., Kania, A., Jessell, T., Behringer, R.R., 1999. *Lim1* is required in both primitive streak derived tissues and visceral endoderm for head formation in the mouse. Development 126, 4925–4932.

Shimono, A., Behringer, R.R., 1999. Isolation of novel cDNAs by subtractions between the anterior mesendoderm of single mouse gastrula stage embryos. Dev. Biol. 209, 369–380.

Shimono, A., Behringer, R.R., 2003. Angiomotin regulates visceral endoderm movements during mouse embryogenesis. Curr. Biol. 13, 613–617.

Srinivas, S., Rodriguez, T., Clements, M., Smith, J.C., Beddington, R.S.P., 2004. Active cell migration drives the unilateral movements of the anterior visceral endoderm. Development 131, 157–164.

Stottmann, R.W., Choi, M., Mishina, Y., Meyers, E.N., Klingensmith, J., 2004. BMP receptor IA is required in mammalian neural crest cells for development of the cardiac outflow tract and ventricular myocardium. Development 131, 2205–2218.

Sturm, K., Tam, P.P.L., 1993. Isolation and culture of whole post-implantation embryos and germ layer derivatives. Methods Enzymol. 225, 164–190.

Suda, Y., Nakabayashi, J., Matsuo, I., Aizawa, S., 1999. Functional equivalency between Otx2 and Otx1 in development of the rostral head. Development 126, 743–757.

Tam, P.P.L., Beddington, R.S.P., 1987. The formation of mesodermal tissues in the mouse embryo during gastrulation and early organogenesis. Development 99 (1), 109–126.

Tam, P.P.L., Beddington, R.S.P., 1992. Establishment and organization of germ layers in the gastrulating mouse embryo. Ciba Found. Symp. 165, 27–41.

Tam, P.P.L., Behringer, R.R., 1997. Mouse gastrulation: the formation of a mammalian body plan. Mech. Dev. 68, 3–25.

Tam, P.P.L., Steiner, K.A., 1999. Anterior patterning by synergistic activity of the early gastrula organiser and the anterior germ layer tissues of the mouse embryo. Development 126, 5171–5179.

Tam, P.P.L., Tan, S.S., 1992. The somitogenetic potential of cells in the primitive streak and the tail bud of the organogenesis-stage mouse embryo. Development 115, 703–715.

Tam, P.P.L., Steiner, K.A., Zhou, S.X., Quinlan, G.A., 1997. Lineage and functional analyses of the mouse organiser. Cold Spring Harbor Symp. Quant. Biol. 62, 135–144.

Tam, P.P.L., Gad, J.M., Kinder, S.J., Tsang, T.E., Behringer, R.R., 2001. Morphogenetic tissue movement and the establishment of body plan during development from blastocyst to gastrula in the mouse. BioEssays 23, 508–517.

Thomas, P., Beddington, R., 1996. Anterior primitive endoderm may be responsible for patterning the anterior neural plate in the mouse embryo. Curr. Biol. 6, 1487–1496.

Tsang, T.E., Shawlot, W., Kinder, S.J., Kobayashi, A., Kwan, K.M., Schughart, K., Kania, A., Jessell, T.M., Behringer, R.R., Tam, P.P.L., 2000. Lim1 activity is required for intermediate mesoderm differentiation in the mouse embryo. Dev. Biol. 223, 77–90.

Tsang, T.E., Khoo, P.-L., Jamieson, R.V., Zhou, S.X., Ang, S.-L., Behringer, R.R., 2001. The allocation and differentiation of mouse primordial germ cells. Int. J. Dev. Biol. 45, 549–555.

Wilkinson, D.G., Nieto, M.A., 1993. Detection of messenger RNA by in situ hybridisation to tissue sections and wholemounts. Methods Enzymol. 225, 361–373.

Yamamoto, M., Saijoh, Y., Perea-Gomez, A., Shawlot, W., Behringer, R.R., Ang, S.L., Hamada, H., Meno, C., 2004. Nodal antagonists regulate formation of the anteroposterior axis of the mouse embryo. Nature 428, 387–392.

Zakin, L., De Robertis, E.M., 2004. Inactivation of mouse Twisted gastrulation reveals its role in promoting Bmp4 activity during forebrain development. Development 131, 413–424.